

# Degradation of anion exchange membranes used for hydrogen production by ultrapure water electrolysis

## Electronic Supplementary Information

Javier Parrondo <sup>a</sup>, Christopher G. Arges <sup>a</sup>, Mike Niedzwiecki <sup>b</sup>, Everett B. Anderson <sup>b</sup>, Katherine E. Ayers <sup>b</sup> and Vijay Ramani <sup>a, \*</sup>

<sup>a</sup> Center for Electrochemical Science and Engineering, Department of Chemical and Biological Engineering, Illinois Institute of Technology, 10 W. 33rd St., Chicago, IL 60616

\*Corresponding author's e-mail: [ramani@iit.edu](mailto:ramani@iit.edu)

<sup>b</sup> Proton Energy Systems, Wallingford, CT 06492, USA

Email: [kayers@protononsite.com](mailto:kayers@protononsite.com)

### *Synthesis of the Anion Exchange Membranes (AEMs)*

#### *Synthesis of chloromethylated polysulfone*

Chloromethylated polysulfone (CMPSF) was synthesized via the Friedel-Crafts reaction. The exact procedure used in our laboratory is a modification of the procedure described by Avram and coworkers <sup>1</sup> and was described in our previously published work.<sup>2</sup> We selected polysulfone (PSF) with a molecular weight of 75,000 g mol<sup>-1</sup> (Acros Organics) for preparing the PSF AEMs.<sup>3</sup>

#### *Synthesis of PSF AEMs*

CMPSF (DF=1.24 – number of chloromethyl groups per polymer repeating unit) was dissolved in extra dry N,N-dimethylformamide (DMF – stored over molecular sieves) to form a 4 to 4.5 wt% solution. Next, a tertiary amine base (trimethylamine (TMA) or 1-azabicyclo[2.2.2]octane (ABCO)) or 1-methylimidazole (1M) was added as limiting reagent to the solution to achieve a theoretical IEC of approximately 1.8 mmol g<sup>-1</sup>. Table S1 below lists the ratio of base reagent to chloromethylated groups to achieve a theoretical IECs of 1.8 mmol g<sup>-1</sup>.

**Table S1.** Ratio of base reagent to chloromethyl groups in CMPSF (DF=1.24) for preparing AEMs with a theoretical IEC of 1.8 mmol g<sup>-1</sup>

AEM material	Ratio of base reagent to chloromethyl groups (mol/mol)
PSF-TMA <sup>+</sup>	0.8:1 Base reagent: 33wt% trimethylamine in ethanol (Acros Organics)
PSF-ABCO <sup>+</sup>	0.9:1 Base reagent: 1-azabicyclo[2.2.2]octane (97% Sigma-Aldrich)
PSF-1M <sup>+</sup>	0.85:1 Base reagent: 1-methylimidazole (99% Acros Organics)

The reaction solutions for preparing PSF-ABCO<sup>+</sup> Cl<sup>-</sup> and PSF-1M<sup>+</sup> Cl<sup>-</sup> were heated to 60°C for 12 hours and the reaction for preparing PSF-TMA<sup>+</sup> Cl<sup>-</sup> was carried-out at room temperature (due to the volatility of TMA) for 48 hours. At the end of the reaction, the solutions were drop cast on to a glass plate on a leveled surface in an oven and the DMF solvent was evaporated by heating to 60°C for at least 12 hours. After drying, a thin-film remained on the glass plate and it was removed by immersion in deionized water and with a knife. The film was then stored in deionized (DI) water (18 MΩ).

Note: To prepare membranes of 40-50 mm by casting on 9 cm × 9 cm glass plates, we used 0.4 to 0.5 g CMPSF dissolved into 9.5 mL of DMF following the aforementioned procedure.

#### ***NMR characterization.***

All the NMR experiments were conducted in a Bruker Avance 360 MHz NMR spectrometer. The <sup>1</sup>H-NMR spectra were collected at 360 MHz. NMR samples were prepared by dissolving at least 30-40 mg of sample in 1 mL of deuterated solvent (d6-dimethylsulfoxide, d6-DMSO). 35 μL of NMR grade tetramethylsilane (TMS) was added as an internal standard to calibrate the chemical shift of the NMR spectrum (δ=0 ppm). Figures S1 and S2 provide the <sup>1</sup>H NMR of PSF and CMPSF.

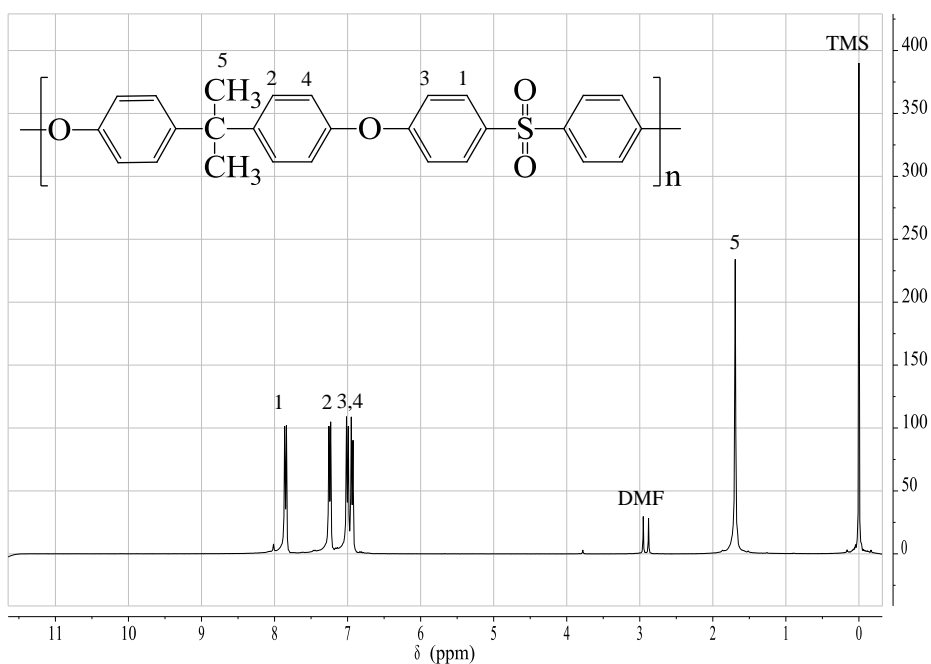


**Figure S1.**  $^1\text{H}$  NMR of polysulfone (PSF).

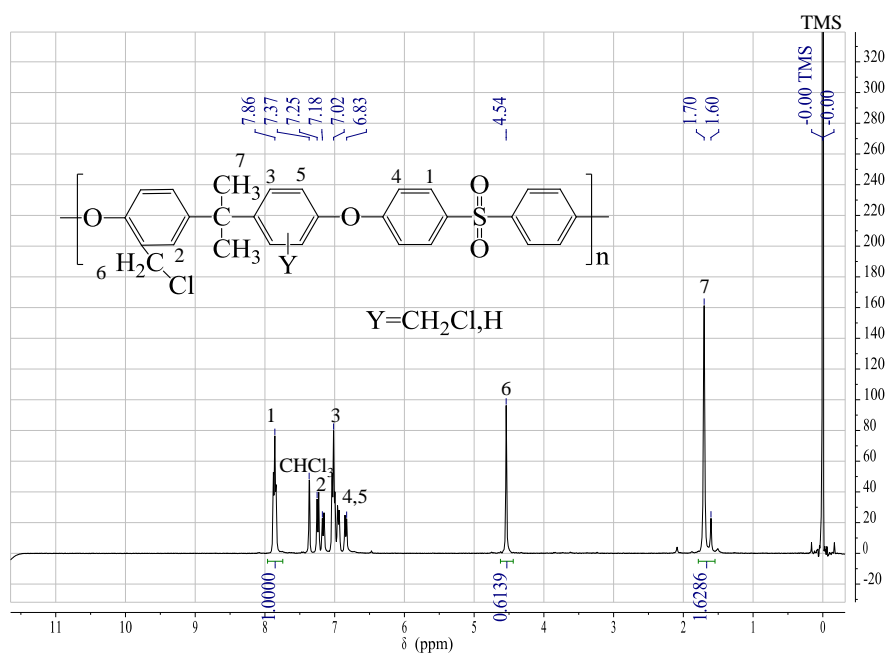


**Figure S2.**  $^1\text{H}$  NMR of chloromethylated polysulfone (CMPSF).  $DF=1.24$ .

The degree of chloromethylation was quantified using the integrated  $^1\text{H}$  NMR spectrum (see equation [1]).

$$DF = \frac{\text{Area}_1 \text{ of H at } \delta = 4.5 \text{ ppm} (-\text{CH}_2 - \text{Cl})}{\text{Area}_0 \text{ of H at } \delta = 1.7 \text{ ppm} (-\text{C}(\text{CH}_3)_2 -)} \times \frac{6}{2} \quad [1]$$

The  $^1\text{H}$  NMR spectra of PSF AEMs are provided in Figures S3 to S5. The in-plane hydroxide ion conductivities of the prepared AEMs are provided in Figure S6. PSF-  $\text{TMA}^+ \text{OH}^-$  had higher conductivity than PSF- $\text{ABCO}^+$

$\text{OH}^-$  and PSF-1M<sup>+</sup>  $\text{OH}^-$  membranes. The lower conductivity of PSF-ABCO<sup>+</sup> could be due to the larger water uptake of AEMs with ABCO<sup>+</sup> and/or the fact that ABCO<sup>+</sup> is conformationally constrained (unlike TMA<sup>+</sup>) resulting in a stronger electrostatic interaction with the hydroxide ion. The PSF-TMA<sup>+</sup> membrane and binder achieved better performance during alkaline water electrolysis at 50°C (See Figure S7), than the membranes functionalized with ABCO<sup>+</sup> or 1M<sup>+</sup>. However, the differences could not be ascribed purely due to the ionic conductivity difference between the membranes, which was relatively small. The impact of CO<sub>2</sub> intrusion, the differences in the degradation rates of these AEMs, and other operational parameters all affect the performance of the electrolyzer. Degradation of anion exchange membranes used for hydrogen production by ultrapure water electrolysis. Additionally, the cation group type has been documented by Varcoe and co-workers to influence the oxygen redox reaction (ORR) in alkaline media<sup>4</sup>; they demonstrated that quaternary benzyl 1-methyl imidazolium cations hindered the ORR in alkaline media more than quaternary benzyl trimethylammonium cations. This effect could have also influenced the performance of the water electrolyzers prepared using the two different AEMs. For these experiments, the thickness of the AEMs used were approximately 50 μm, and the cell resistances were 0.60 Ohm-cm<sup>2</sup> for the TMA<sup>+</sup> based water electrolyzer and 0.72 Ohm-cm<sup>2</sup> for the ABCO<sup>+</sup> based water electrolyzer.

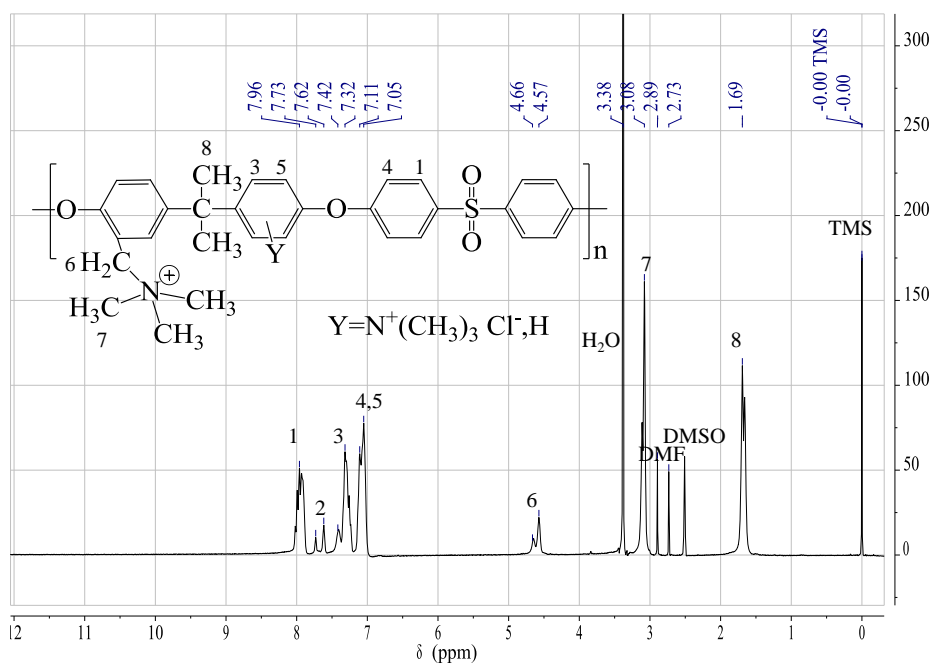


Figure S3. <sup>1</sup>H NMR of PSF-TMA<sup>+</sup> Cl<sup>-</sup>.

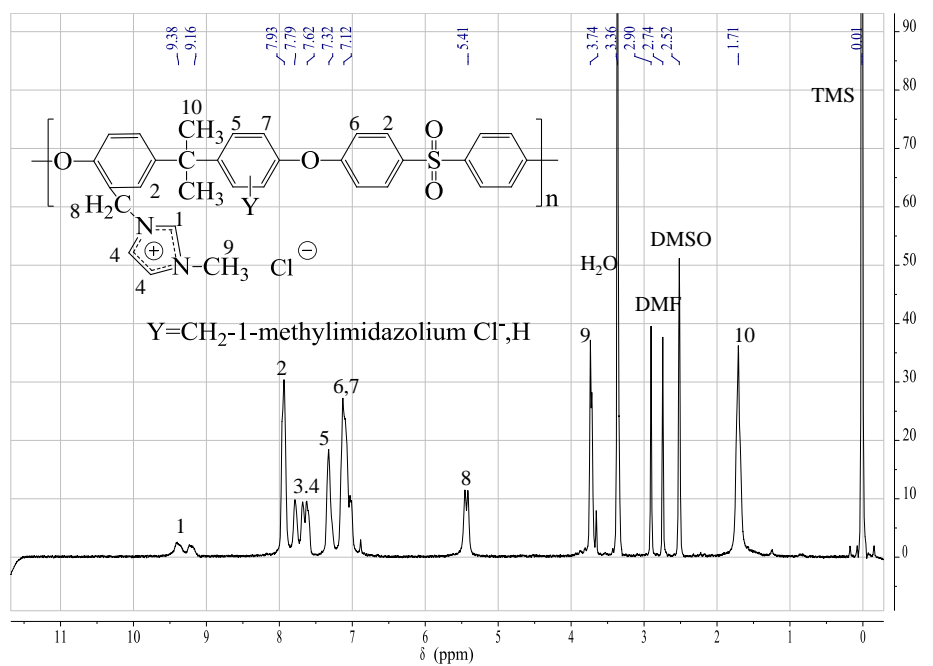


Figure S4. <sup>1</sup>H NMR of PSF-1M<sup>+</sup> Cl<sup>-</sup>.

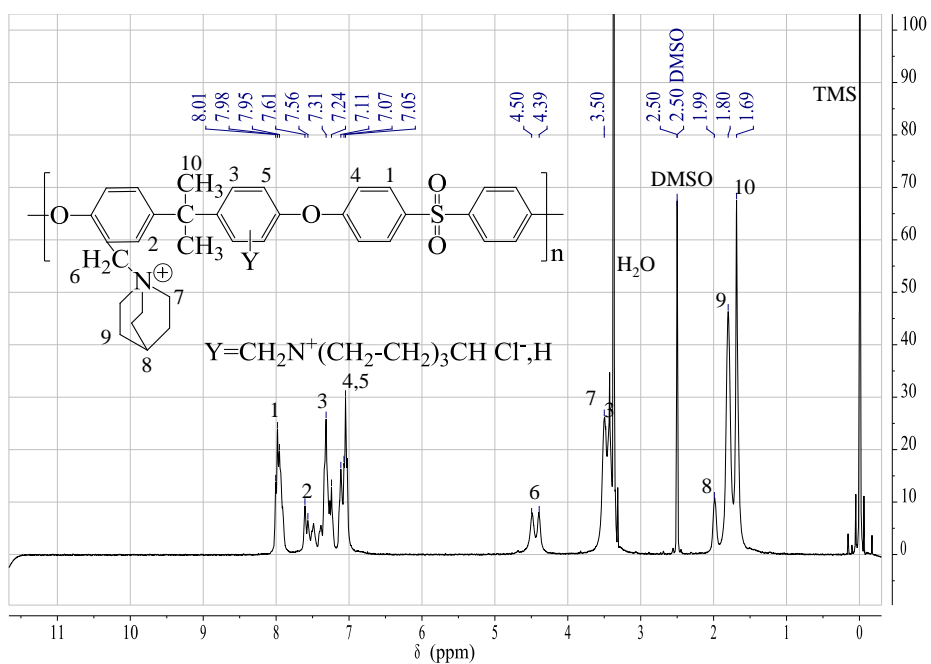


Figure S5.  $^1\text{H}$  NMR of PSF-ABCO $^+$  Cl $^-$ .

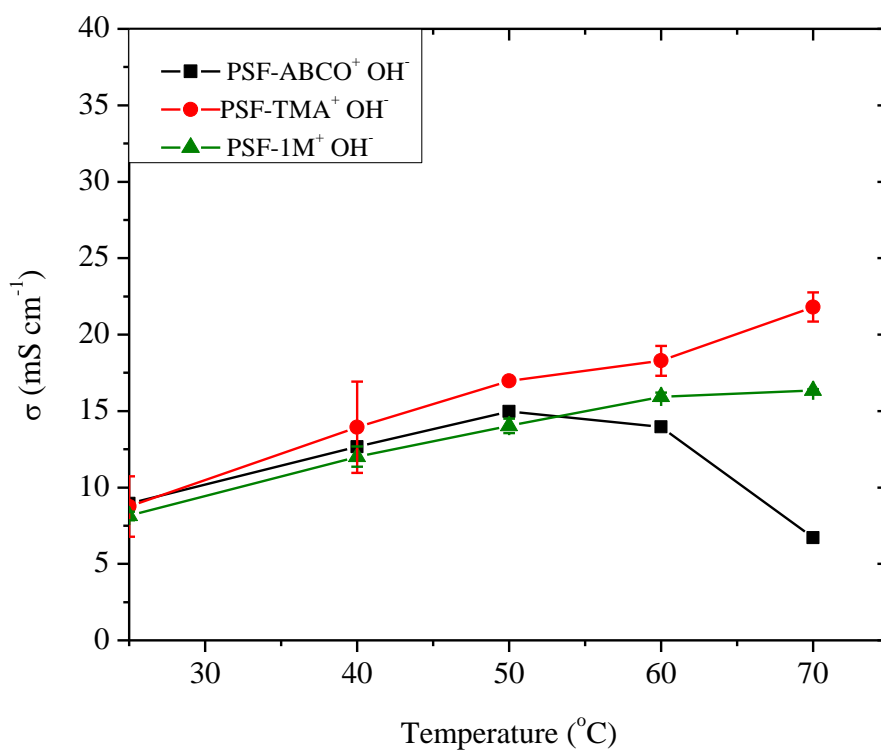
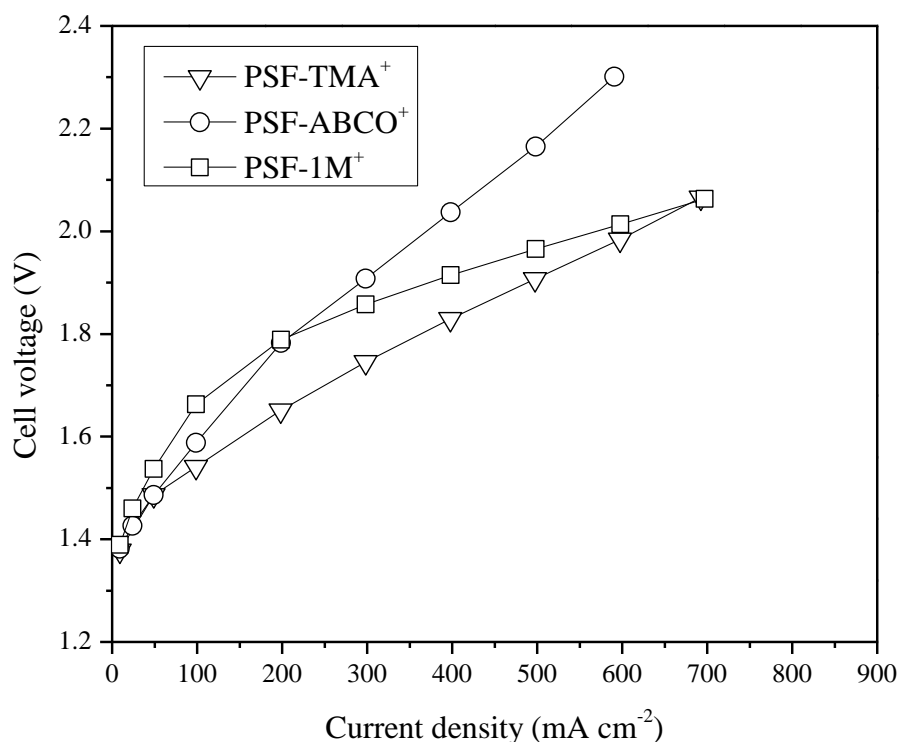


Figure S6. In-plane hydroxide ion conductivity of PSF AEMs prepared from CMPSF (DF=1.24).



**Figure S7.** Polarization curves for alkaline water electrolysis at 50°C using PSF AEMs functionalized with different cation groups.

#### *Alkaline membrane electrolyzer operation.*

Ultrapure water (18 M $\Omega$  prepared by Millipore Direct Q5 – drawn fresh daily) electrolysis was carried out in a 25 cm<sup>2</sup> single fuel cell hardware (Fuel Cell Technologies, Inc). The anode graphite plate was replaced by a corrosion resistant metal plate (with 2 mm x 2 mm single serpentine flow fields) to avoid carbon corrosion as a consequence of the elevated voltages used to electrolyze water. Membrane electrode assemblies (MEAs) with an active area of 25 cm<sup>2</sup> were assembled in the hardware by placing an AEM between two gas diffusion electrodes (without heating or pressing).

The cathode (hydrogen evolution electrode) gas diffusion electrode (GDE) was prepared by applying platinum (Pt) black electrocatalyst onto a carbon paper GDL (Sigracet® GDL 10BC) using an airbrush. The Pt black loading was approximately 2.5 mg/cm<sup>2</sup>; the binder (PSF-TMA<sup>+</sup> Cl<sup>-</sup>, PSF-ABCO<sup>+</sup> Cl<sup>-</sup> or PSF-1M<sup>+</sup> Cl<sup>-</sup>) concentration was 30 wt% (dry weight). Similarly, the anode GDE was prepared by applying (using an airbrush) an ink containing the electrocatalyst (lead ruthenate pyrochlore) and binder onto a porous media electrode. The electrocatalyst loading was approximately 2.5 mg/cm<sup>2</sup>; the binder (PSF-TMA<sup>+</sup> Cl<sup>-</sup>, PSF-ABCO<sup>+</sup> Cl<sup>-</sup> or PSF-1M<sup>+</sup> Cl<sup>-</sup>) concentration was 30 wt% (dry weight).

The electrodes and the membrane were prepared with the AEMs in the chloride counter ion form. The membrane electrode assembly was ion exchanged to hydroxide form (required for the proper operation of the electrolyzer) by immersing in 1 M KOH at room temperature overnight, followed by washing with excess deionized (DI) until neutral pH was achieved. The latter step removed the excess KOH from the membrane electrode assembly.

The water was fed to the anode and recirculated to the storage tank, which was maintained at 50°C, at a flow rate of approximately 0.4 L min<sup>-1</sup>. Previous experiments have shown that feeding the water through either only the anode or through both anode and cathode does not impact the electrolyzer performance. The water can diffuse through the membrane and reach the cathode, where it electrochemically splits into hydrogen and hydroxide. The absence of water feed at the cathode makes it easier to recover the hydrogen produced and simplifies the production of dry hydrogen at elevated pressures.

Nitrogen was bubbled continuously through the storage tank to minimize carbon dioxide dissolution in the ultrapure water. We also found that carbon dioxide could diffuse inside the MEA through the hydrogen exit tube. In some experiments, the cathode side was isolated from the carbon dioxide in the air by keeping the hydrogen exit tube immersed in 1M KOH solution. Carbon dioxide is very soluble in concentrated alkaline solutions and therefore it will dissolve in the KOH solution to form carbonate species, thereby preventing its ingress into the cell. Polarization curves were obtained by stepping the current density from 10 mA cm<sup>-2</sup> to 700 mA cm<sup>-2</sup> (10, 25, 50, 100, 200, 300, 400, 500, 600 and 700 mAcm<sup>-2</sup>). The system was held at each current density for 2 minutes. The acquisition was stopped when the voltage rise above 2.5 V.

### ***Synthesis and characterization of lead ruthenate pyrochlores (Pb<sub>2</sub>Ru<sub>2</sub>O<sub>6.5</sub>)***

Pyrochlore compounds can be represented by the general formula [A<sub>2</sub>O']<sub>2</sub>[B<sub>2</sub>O<sub>6</sub>]<sub>3</sub>, consisting in a network of corner sharing BO<sub>6</sub> octahedra, with A and O' atoms occupying interstitial sites.<sup>5</sup> A is usually a lanthanide or non-metal and B a transition metal cation. When polarizable cations such as Pb<sup>2+</sup> and/or Bi<sup>3+</sup> occupy the A site, the resulting pyrochlores have metallic conductivity (which allows the preparation of self-supported OER electrodes).

Lead ruthenate pyrochlores were synthesized following the alkaline solution technique described initially by Horowitz and coworkers.<sup>6</sup> Ruthenium (III) chloride hydrate (5 mmol, RuCl<sub>3</sub>, 35-40% Ruthenium, Acros) and lead acetate trihydrate (5 mmol, Pb(C<sub>2</sub>H<sub>3</sub>O<sub>2</sub>)<sub>2</sub>, 99%, Aldrich) were dissolved in approximately 50 mL DI water and



stirred for 20 minutes. The salt mixture was precipitated in 500 mL of O<sub>2</sub>-saturated 4M KOH and kept in the same KOH solution at 85°C with continuous oxygen bubbling for 5 days to allow the amorphous precipitate to crystallize. Then, the solid was recovered by centrifugation and washed with DI water until neutral pH was attained, treated with glacial acetic acid to remove any lead oxide impurities (Aldrich, 98%) and then washed 5 times with acetone. Finally, the solid was dried using supercritical carbon dioxide (4,000 psi, 45 °C) to get a high surface area electrocatalyst. XRD pattern of the lead ruthenate electrocatalyst obtained using this procedure shows the presence of crystalline pyrochlore (Figure S7). The peaks associated with Pb<sub>2</sub>Ru<sub>2</sub>O<sub>6.5</sub> can be seen at 2θ values of 30°, 35°, 50°, 59, 62°, 73°, 81° and 84° representing the (222), (400), (440), (622), (444), (800), (662) and (840) Bragg's reflections of the cubic (space group: Fd-3m) structure of the pyrochlore.

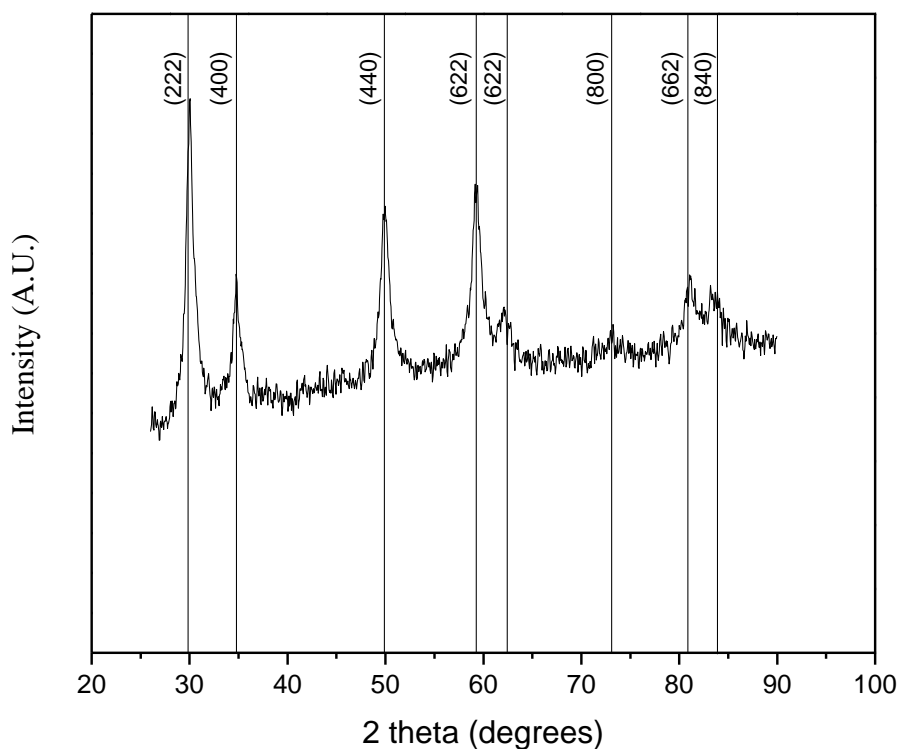


**Figure S8.** XRD spectrum of lead ruthenate pyrochlore.

### Impedance spectra acquired during electrolyzer testing

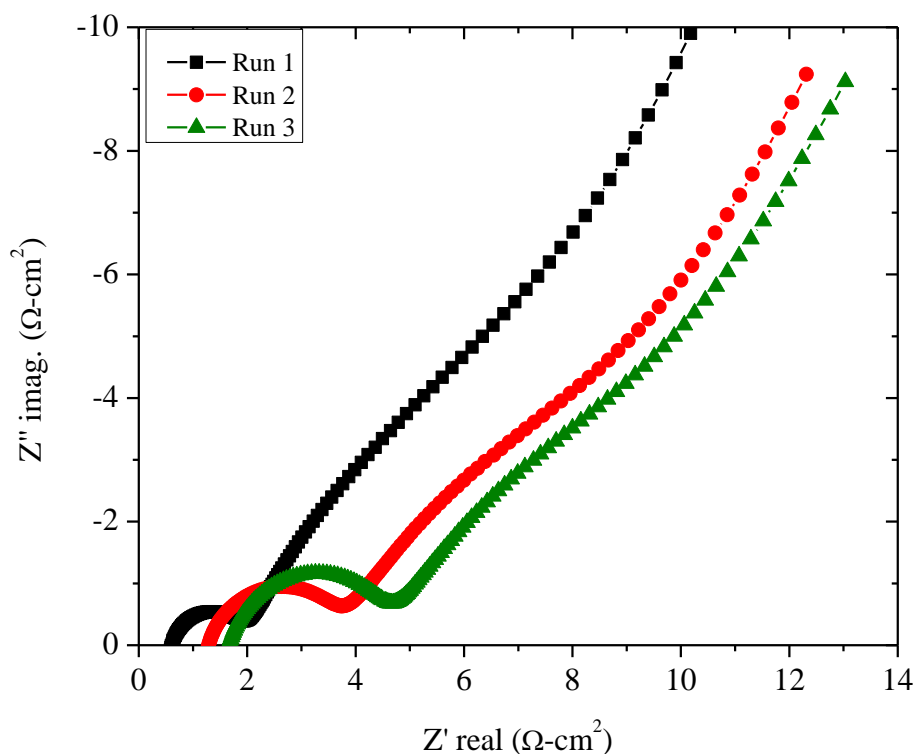


**Figure S9.** Electrochemical impedance spectroscopy acquired after recording polarization curves (runs 1, 2 and 3). The spectra correspond to the polarization curves shown in Figure 2 of the manuscript. This figure is used to demonstrate the effect of carbon dioxide intrusion on the resistances within the electrolyzer membrane electrode assembly. Over time, the high frequency resistance (HFR) increased from 0.60 to 1.67 ohm-cm<sup>2</sup>. The charge transfer resistance also increased by over 3-fold during this experiment.

### Continuous electrolyzer operation

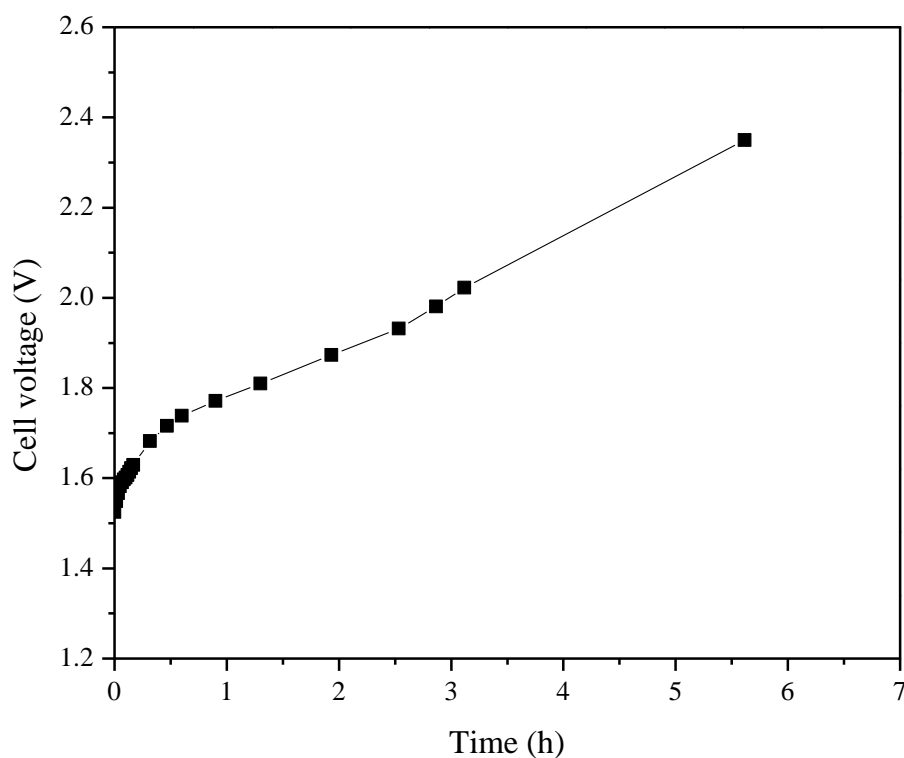


**Figure S10.** Stability test using PSF-TMA<sup>+</sup>OH<sup>-</sup> MEA. The electrolyzer was run at 200 mAcm<sup>-2</sup> and 50°C using ultrapure water continuously 6 h. Cathode: electrocatalyst loading, 2.5 mg Pt black/cm<sup>2</sup>; 30wt% ionomer (PSF-TMA<sup>+</sup>OH<sup>-</sup>). Anode: electrocatalyst loading, 2.5 mg Pb<sub>2</sub>Ru<sub>2</sub>O<sub>6.5</sub>/cm<sup>2</sup>; 30wt% ionomer (PSF-TMA<sup>+</sup>OH<sup>-</sup>).

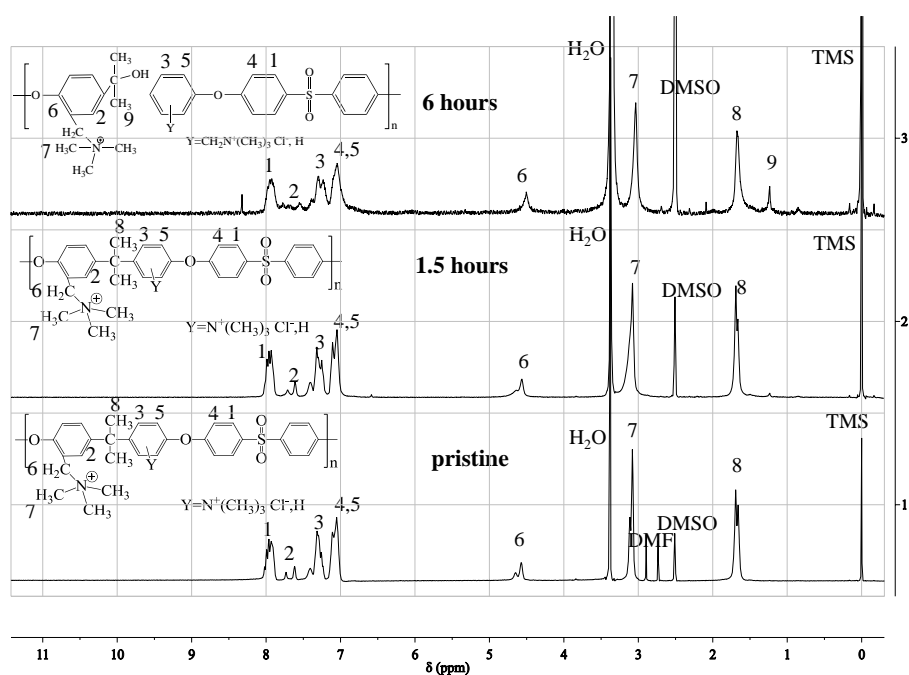


**Figure S11.**  $^1\text{H-NMR}$  (0 to 11.5 ppm) of pristine (before use in water electrolyzer) and post-mortem AEM water electrolyzer samples after acquisition of 3 polarization runs (approximately 1.5 hours of continuous operation) and after continuous operation at  $200\text{ mA cm}^{-2}$  for 6 hours.

## References

1. E. Avram, E. Butuc, C. Luca and I. Druta, *J. Macromol. Sci., Part A: Pure Appl. Chem.*, 1997, **A34**, 1701.
2. C. G. Arges, J. Parrondo, G. Johnson, A. Nadhan and V. Ramani, *J. Mater. Chem.*, 2012, **22**, 3733.
3. C. G. Arges and V. Ramani, *Proc. Natl. Acad. Sci. U. S. A.*, 2013, **110**, 2490.
4. A. L. Ong, D. K. Whelligan, M. L. Fox and J. R. Varcoe, *Physical Chemistry Chemical Physics*, 2013, **15**.
5. R. A. McCauley, *J. Appl. Phys.*, 1980, **51**, 290.
6. H. S. Horowitz, J. M. Longo, H. H. Horowitz and J. T. Lewandowski, *ACS Symp. Ser.*, 1985, **279**, 143.